Optical conductivity the optical conductivity resonance from an exact description of the electronic states around the Fermi energy

F. Puch

Departamento de Física, Universidad de Zacatecas, Zacatecas, México.

R. Baquero

Departamento de Física, CINVESTAV, Apartado Postal 14-740, México D.F.

In this paper we show that the optical conductivity can be calculated to agree with experiment if the details of the electronic states around the Fermi level are taken into account with some care. More precisely, we present a calculation of the optical conductivity in $YBa_2Cu_3O_7$ on the basis of an exact (*ab initio*) three dimensional electronic band structure calculation from which we extract the information on the bands near the Fermi energy that can be associated with the CuO_2 plane-carrier states. To simulate the superconducting state, we superimpose a gap on these bands alone. On these basis, from the known Kubo-Greenwood formula we calculate the optical conductivity in the normal and in the superconducting state. Our calculation agrees with the experimental result even in the higher part of the frequency spectrum. Our way of calculating the resonance suggests a model of evolution for the bands under the effect of doping consistent with the recent experimental findings that the optical resonance can disappear while the sample remains superconducting. An important conclusion of this paper is that the resonance depends mostly on the details of the electronic band structure. It is enough to take into account the effect of the superconducting transition through a single parameter (the gap). No details on the mechanism are needed, so no mechanism can be tested on this basis. Our calculation suggests a model of evolution for the bands around the Fermi energy under doping that gives some microscopic foundations to the recent experiments that show unambiguously that the resonance cannot be the cause of superconductivity. Most importantly, it indicates how the background is built up and depends on the electronic excitations accessible through values of the energy transfer on a wider interval than the one contributing directly to the resonance. These electronic excitations are determined by the optical transitions allowed. From this point of view, it is an obvious consequence that the background is with small differences, common to all the cuprates having a CuO_2 plane. But the most important conclusion is that the background contains essentially the same physics as the resonance does, and so it does not have any detailed information on the superconducting mechanism as well, contrary to the conclusions of recent work.

Keywords: Superconductivity, mechanism, $YBa_2Cu_3O_7$, Optical Conductivity, resonante.

En esta carta mostramos que la conductividad óptica puede calcularse con base en el cálculo detallado de los estados electrónicos reales en las cercanías del nivel de Fermi. Más exactamente, presentamos aquí el cálculo de la conductividad óptica para el material superconductor $YBa_2Cu_3O_7$ basado en un cálculo tridimensional *ab initio* en el cual hemos identificado las bandas que pueden asociarse al plano de CuO_2. Para simular el estado superconductor, imponemos a mano una brecha a esas bandas exclusivamente. Nuestro cálculo es pues bidimensional pero usa información de un cálculo tridimensional. Usamos la conocida fórmula de Kubo-Greenwood, sin hacer uso de la brecha para obtener el cálculo en el estado normal e imponiendo la brecha en la forma descrita para el estado superconductor. Ambos resultados se ajustan muy bien con los experimentos conocidos incluso en la parte alta del espectro. Nuestra forma de calcular sugiere un modelo para la evolución de las bandas en función del contenido de oxígeno que es consistente con el hallazgo reciente de que la resonancia desaparece antes de que la muestra deje de ser superconductora. Una conclusión importante de este trabajo es que la resonancia depende en forma muy directa de los detalles de la estructura de bandas y, por lo tanto, no incluir esos detalles, tiene un efecto quizás irremediable. Por otro lado, el modelo muestra que la superconductividad misma, puede ser bastante simple. Fue suficiente incluir un solo parámetro, la brecha, sin hacer referencia a ningún mecanismo, para obtener el resultado. Este cálculo sugiere un modelo para la evolución de las bandas con el contenido de oxígeno que le da un fundamento microscópico a los experimentos recientes y que muestra, por el contrario, que la resonancia no puede explicar el mecanismo. Lo mismo vale para el ruido de fondo al cual se le atribuyó importancia, en este sentido, recientemente. Más importante aun, este cálculo muestra como el ruido de fondo está determinado por las transiciones ópticas permitidas en las frecuencias aledañas a la resonancia. Todas vienen del plano de CuO_2 y, en ese sentido, es normal que el ruido de fondo sea, detalle más, detalle menos, común a todos los cupratos. Pero la conclusión más importante es que el ruido de fondo no contiene ninguna información sobre el mecanismo, conclusión que es contraria a la de algunos trabajos recientes.

Descriptores: Superconductividad; mecanismo; $YBa_2Cu_3O_7$; conductividad óptica; resonancia.

PACS: 74.20-z; 74.25.Gz; 74.72.Bk

1. Introduction

J. Hwang, T.Timusk, and G.D. Gu [1] have reported an infrared spectroscopy study of optical conductivity as a function of doping in various samples of Bi-2212. The effect of doping into Bi-2212 is to lower both the critical temperature, T_c, and the intensity of the resonance peak that appears in the superconducting state. This fact represented a unique opportunity to separate the resonance from the mechanism of superconductivity by means of a direct experiment. These authors have reported the fabrication of several superconducting samples of Bi-2212 with different doping content up to a

particular one with 0.23 holes per Cu atom that resonance. Its high critical temperature (Tc=55K) demonstrates that superconductivity in this sample is still robust. This experimental fact leads to the important conclusion that resonance cannot be taken as the cause of superconductivity. Nevertheless, since resonance appears in the superconducting and only in the superconducting state, it should be somehow tightly bound to the phase transition itself.

A resonance peak [2,3] also appears in the spin polarized magnetic susceptibility, $\chi_s(\omega)$, at a frequency, ω_{res}, that is characteristic of the specific sample. The magnetic resonance peak appears as a common excitation to the superconducting state of all high-Tc superconductors investigated by Inelastic Neutron Scattering (INS) so far with a maximum $T_c \approx 90$K. The existence of the excitation does not depend on the number of CuO_2 planes per unit cell: one for $Tl_2Ba_2CuO_{6+\delta}$, two for $YBa_2Cu_3O_{6+\delta}$ and $Bi_2Sr_2CaCu_2O_{8+\delta}$. It has never been observed in the monolayer system $La_{2-x}Sr_xCuO_4$ with maximum Tc ≈ 40K [4]. Although there are several proposals in the literature [4] to associate the origin of the resonance with a mode of magnetic origin, we want to point to a direct and simple relation between the effect that the superconducting phase transition has on the electronic band structure, and the resonance itself.

In their paper above quoted, J. Hwang, T. Timusk and G.D. Gu present the optical single-particle self-energy which is directly related to optical conductivity. They call the resonance that they find "the resonance optical mode". This resonance optical mode in the optical conductivity, $\sigma_{opt}(\omega)$, is produced at the same characteristic frequency, ω_{res}, as in the susceptibility. Both resonances differ on details, however. It is important to note that the two thermodynamic functions can be considered mutually exclusive in the sense that, while the non-zero contributions to the matrix elements in the spin polarized susceptibility are intra-band, in the optical conductivity these are inter-band transitions. In that sense it might appear at first sight surprising that the two resonances have the same origin. Carbotte *et al.* [5] assumed that the resonance in $\chi_s(\omega)$ can be related to the effective spectrum of the spin fluctuations, and used it to construct the Eliashberg function of the conventional theory of superconductivity from which all the information on thermodynamics follows [6]. They have used this knowledge to calculate the resonance in the optical conductivity, $\sigma_{opt}(\omega)$, in the superconducting state. Their result agrees with experiment. They further used an inversion procedure [7] that allows them to extract information about the Eliashberg function from optical conductivity. In this way they got back their assumed Eliashberg function (directly related to $\chi_s(\omega)$ in their work). The procedure used by Carbotte *et al.* establishes an essentially common origin to the resonance in both thermodynamic functions (not to the functions themselves). Since the experiments by J. Hwang *et al.* [1] clearly show that the resonance in the optical conductivity is not responsible for superconductivity, it is natural to expect that the resonance in the susceptibility will not be responsible for superconductivity either,

and therefore cannot be directly related to the real Eliashberg function. But an important point is that Carbotte *et al.* show explicitly that the resonances in both functions have a common origin. Resonance has been the object of a substantial amount of work in the last few years [5, 8–19].

ARPES experiments by Lanzara *et al.* [20] have shown that a "kink" in the kinetic energy spectra of several cuprate superconductors reveals a coupling of the carriers to the intermediate boson that causes the superconducting transition. They have attributed it to phonons. Other researchers have attributed it rather to a coupling to a magnetic mode [5,21–23]. A more recent paper by Lanzara *et al.* [24] emphasizes the same previous conclusion: the intermediate boson is a phonon. It is clear [1] that the optical self-energy as measured by infrared is somehow related to the quasiparticle self-energy as measured in ARPES experiments but they are not identical, and there are important differences in the two quantities [25].

To calculate the optical conductivity in $YBa_2Cu_3O_7$, we start from an *ab initio* LAPW three dimensional (3D) calculation of the electronic band structure [26–28]. When we compared the band structure calculations in the literature, we found that there is a certain disagreement on the exact description of the bands around the Fermi level, E_F. To improve our results according to experiments and to the accepted information on the bands around the Fermi level, we found it useful to fit our 3D *ab initio* bands to a tight-binding Hamiltonian. This allows us to slightly fine-tune our bands around the Fermi level (see below).

We next calculate the optical conductivity, $\sigma_{opt}(\omega)$, in the normal state for $YBa_2Cu_3O_7$ from the known Kubo-Greenwood formula [29] and compare the result with our experiment [28]. For that purpose, we have identified the electronic bands of the carriers associated with the CuO_2 plane. We then perform the same calculation in the superconducting state. To simulate the superconducting state, we have introduced into the electronic band structure a superconducting gap in the bands that describe the carriers on the CuO_2 plane and only in them. We perform the calculation using the same formula and our built up "superconducting band structure". Resonance appears in the superconducting and only in the superconducting state, at $\omega_{res} = 2\Delta = 38 meV$ (Δ is the gap that we used for the CuO_2-plane carrier-bands). So we argue that the superconducting phase transition effectively modifies the electronic bands around the Fermi level and that this feature opens up several new channels for allowed transitions with energy transfer $\omega_{res} = 2\Delta$ and thus produces the experimentally observed effect. We will show below how both the intra- and inter-band transitions are projected by the superconducting phase transition to the same energy 2Δ, a fact that explains the common origin of the resonance in both thermodynamic functions.

The model that we present here has the advantage that, on exactly the same footing, it accounts for several experimental results of different characters [30]. We will comment on this further below. We deal in this paper with $YBa_2Cu_3O_7$.

Our model sharply separates the cause of the resonance from the cause of superconductivity as the infrared experiments [1] indicate. The resonance arises from the effect that the superconducting transition (the gap) has on the electronic band structure, but superconductivity (the gap itself) can arise from whatever mechanism. Further, to the extent to which we can account for the resonance by taking only the gap value as the information on the superconducting state, it is clear that no information on the specific mechanism can be obtained from it. It appears that the resonance does not contain enough information on the superconducting mechanism to be useful to decide on it.

The background is built up from the allowed transitions at energies different from ω_{res}. The physics that it contains is essentially the same. No information on the mechanism can be extracted from the background either, since it appears that the main contribution to the optical conductivity comes from the optical allowed transitions determined by the electronic states around the Fermi energy and by the influence that the superconducting phase transition (solely through the gap value) has on them. The background as a source of information on the mechanism has been suggested by Hwang *et al.* [1] solely on the basis that it is common to all HTSC. It has been further emphasized by Norman [31]. As it appears to us, neither the resonance nor the background in the optical conductivity can be used effectively to decide on the mechanism of HTSC.

The situation seems not to be the same with the "kink" in the self-energy found in the ARPES experiments [20]. The kink does reveal a coupling and most probably is the key to the superconducting mechanism. Carbotte *et al.* [25] have argued that the ARPES experiments can be interpreted as supporting either spin-fluctuations or the phonon-mediated mechanism. They eliminate the possibility of a phonon-mediated mechanism on the basis of their own calculation of the optical conductivity, assuming this mechanism gives a wrong dependence of this function at high frequencies. As we shall see below, our model gives the correct high-frequency dependence of the optical conductivity. We do not assume any mechanism; we only introduce a detailed description of the electronic bands. At this point it is worth quoting the work by Phillips [32], who argues that the carrier lifetimes are consistent with a phonon mechanism. Nevertheless, we want to point that our work does not prove or favor any mechanism whatsoever. We go backwards instead. We start from the result (the gap) that, if taken from a theoretical formulation, would make it consistent with the thermodynamics of HTSC according to experiment. We deal here with a particular experiment and with a particular HTSC.

The rest of this letter is organized as follows. In Sec. 2, we present our electronic band structure and compare it with other work in the literature. We also include at this point our description of the superconducting state. In Sec. 3, we calculate the optical conductivity for $YBa_2Cu_3O_7$ in the normal and in the superconducting state, and analyze our result. In Sec. 4, we show that our model leads directly to a sugges-

tion for the approximate way in which the electronic band structure might develop around the Fermi Energy under doping for the observed property to emerge quite naturally (the resonance disappears while superconductivity remains). In the final Sec. 5, we put our model in perspective and draw our conclusions. At this point we make some experimental suggestions that might contribute to proving the usefulness of our model. In particular, we suggest that there is no reason for the two resonances to disappear at the same doping concentration. The "kink" in the ARPES experiments should remain as long as the sample remains superconducting regardless of whether it presents one, two or no-resonance at all; only then would it be the key experiment to revealing the mechanism.

2. The Normal and the superconducting state of $YBa_2Cu_3O_7$

2.1. The Electronic Band Structure

The 3D-electronic band structure of $YBa_2Cu_3O_7$ has been calculated by different *ab initio* methods and by the tight-binding method [26, 27, 33–41]. When we compare the different results in the literature, we find that there are differences. The exact position of the bands can differ by as much as 100 meV. These are important differences on the scale of meV which is the proper scale for describing the effect of the superconducting gap.

We first made an *ab initio* LAPW calculation of the normal-state electronic band structure using the WIEN97 code and the parameters of reference [39]. We found it useful to further fit our calculation to a tight-binding description as well as to analyze some details of it [26, 27]. We have paid special attention to the description of the bands near the Fermi energy. For example, we took care that the extended van Hove singularity around the high symmetry point Y [42]
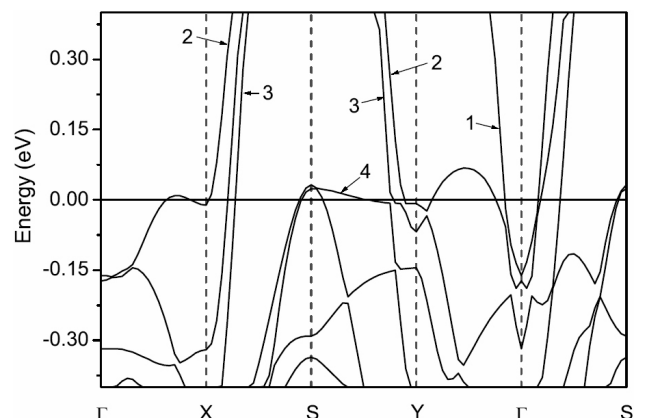
FIGURE 1. 3D-electronic band structure of $YBa_2Cu_3O_7$ near the Fermi level. Bands 2 and 3 are in-CuO_2-plane states; bands 1 and 4 belong to in-CuO-chain states. Notice that the dispersion in the interval S-X is not very different from the one in the interval S-Y for the bands labelled 2 and 3 (the in-CuO_2-plane states). This is not true for bands labelled 1 and 4 that are in-CuO-chain states. The X-Y symmetry is not expected in this scenario.

FIGURE 2. The total density of states (a) and the contribution of each scenario (b).

2.2. Description of the superconducting state

By whatever mechanism, the superconducting transition has the effect of introducing a gap at the Fermi energy, E_F, on the electronic states of the carriers affected by it. Since the actual mechanism is still unknown, we do not try to introduce any. So, to simulate the superconducting phase transition, we have introduced by hand a constant gap, Δ, into our normal-state electronic band structure in the bands near E_F that can be associated with electronic states that belong to the CuO_2 plane. It is important to mention at this point that this model allows us to reproduce right away the optical conductivity and the spin polarized susceptibility on exactly the same basis, both in the superconducting and normal state ($\Delta = 0$). This point is important since, as we have already recalled, these thermodynamic functions seem to exclude each other in the sense that the transitions contributing to their corresponding matrix elements are inter-band in the first case and intra-band in the second. We present the calculation of the spin magnetic susceptibility in detail elsewhere [47], as well as the calculation of the tunnelling characteristics [48]. Here we merely wish to state that these two other results agree with the known experiments.

We have introduced the gap into the electronic band structure in a way that is familiar in BCS theory [49]. Thus, we have removed the states that can be associated wite the CuO_2 plane from the energy interval (E_F-Δ, E_F+Δ) . The states above E_F accumulate at the upper edge of the interval and the ones below at the bottom. Were we to introduce the gap in another way (d-symmetry, for example), the result would differ noticeably from the experimental result. We discuss this point in detail elsewhere [50]. We emphasize that we introduced a gap only to the bands formed by electronic states that can be associated with the atoms belonging to the CuO_2 plane. In this way we obtained what we call the "superconducting electronic band structure" for the CuO_2 plane. In what follows we make use of our tight-binding fit to our own *ab initio* calculation to calculate the optical conductivity.

One more remark is useful. Any complete theory of high-Tc superconductivity should offer an explanation for the two resonances (in the optical conductivity and the spin polarized susceptibility) to occur at the same frequency. Notice that in our model both, intra-band and inter-band transitions are heavily favoured by the phase transition at $\omega_{res} = 2\Delta_{plane}$. But also notice that the events that contribute to the optical conductivity differ from those contributing to spin susceptibility. So the two resonances need neither be equal as a function of ω around ω_{res} nor disappear at the same oxygen content. We refer here to the experiment by J. Hwang, T.Timusk and G.D. Gu [1], where the resonance in the optical susceptibility has been proven to disappear while the sample is still superconducting. That particular sample ($T_c = 55K$) could either show a spin magnetic resonance or could have lost it at higher oxygen content. This experiment has not yet been performed to the best of our knowledge.

should lie at 14 meV below the Fermi energy, in agreement with experiment [43]. Also a van Hove singularity at about -200 meV at $\mathbf{k} = (0.42\pi/a, 0.13\pi/b, 0)$, which has been reported in Ref. 27, was accurately fitted. The overall features of our calculation coincide well with the rest of the other works in the literature. We reproduce our result for the bands around the Fermi energy in Fig. 1. In this figure, the bands labelled 1 and 4 belong to in-CuO-chain states, while those labelled 2 and 3 describe in-CuO_2-plane states. Notice that bands 2 and 3, which belong to the planes, do not show a significantly different dispersion from **S-X** than they do from **S-Y,** while bands 1 and 4, which belong to the chains, do have a different dispersion. In the upper part of Fig. 2, we present the total density of states (DOS) that we get from our band structure. We have obtained a very similar result by calculating it through the Green's function [44] or using the tetrahedral method of integration [45,46]. In the lower part of the same figure, we present the DOS discriminated for each scenario (planes, chains and c-axis). At the Fermi level, their relative contribution is 74% (planes), 15% (chains) and 10% (c-axis). The most important contribution by far comes from the CuO_2-plane states, as is well known.

3. Calculation of optical conductivity

The dielectric function, $\epsilon = \epsilon_1(\omega) + i\epsilon_2(\omega)$ characterizes the optical properties of a material. Experimentally, it can be obtained from the reflectance spectrum. The real and imaginary parts of it are related through the Krammers-Kronig relations. The imaginary part of the dielectric function is directly related to the optical conductivity as

$$\epsilon_2(\omega) = \frac{4\pi\sigma_{opt}(\omega)}{\omega}.$$

For inter-band transitions, we can calculate the optical conductivity from the *Kubo-Greenwood* formula [29]

$$\sigma(\omega) = -\frac{\pi e^2 h^2}{m^2\omega\Omega}\sum_{l,n}\int dk P_{\ln}^i P_{nl}^j f_n(\mathbf{k})[1 - f_l(\mathbf{k})]$$

$$\times\delta(E_l(\mathbf{k}) - E_n(\mathbf{k}) - h\omega), \quad (1)$$

where

$$P_{\ln}^i = \langle\Psi_l(\mathbf{k})|\frac{\partial}{\partial x_i}|\Psi_n(\mathbf{k})\rangle \quad (2)$$

is the optical transition matrix. $|\Psi_n(\mathbf{k})\rangle$ is the Bloch function for the n-band and $\mathbf{k}$ is the wave vector defined in the first Brillouin zone (FBZ). $E_n(\mathbf{k})$ is the corresponding band energy, $f_n(\mathbf{k})$ is the Fermi-Dirac distribution function, ω is the frequency of the radiation and Ω is the volume of the unit cell. The rest are known constants. Now we expand the Bloch function in term of orbital functions as

$$|\Psi_n(\mathbf{k})\rangle = \frac{1}{\sqrt{N}}\sum_{\alpha,j} u_{n,\alpha} e^{i\mathbf{k}\cdot\mathbf{r}_j}|\varphi_\alpha(\mathbf{r} - \mathbf{r}_j)\rangle, \quad (3)$$

where N is the number of unit cells, $\varphi_\alpha(\mathbf{r} - \mathbf{r}_j)$ is the orbital wave function with quantum numbers α, and $\mathbf{r}_j$ is the origin of the j-th unit cell. The $u_{n,\alpha}$ are the coefficients of the expansion. Substituting Eq. 3 into Eq. 2, we get

$$P_{\ln}^i = \sum_{\alpha,\beta} u_{l,\alpha} u_{n,\beta} \sum_{m,j} M_{ijm}^{\alpha,\beta} e^{i\mathbf{k}\cdot(\mathbf{r}_j - \mathbf{r}_m)} \quad (4)$$

with

$$M_{ijm}^{\alpha,\beta} = \langle\varphi_\alpha(\mathbf{r} - \mathbf{r}_m)|\frac{\partial}{\partial x_i}|\varphi_\beta(\mathbf{r} - \mathbf{r}_j)\rangle. \quad (5)$$

The matrix element, Eq. 5, is zero except for in-site and the first nearest neighbors' transitions. $M_{ijm}^{\alpha,\beta}$ can be calculated from our tight-binding fit if we use an approximation suggested by Harrison [51]. Within this approximation, for intersite transitions (atom at $\mathbf{r}_j$ with atom at $\mathbf{r}_i$), $M_{ijm}^{\alpha,\beta}$ can be clast proportional to x_m/d^2, where x_m is the m-component of the vector $\mathbf{r}_j - \mathbf{r}_i$ and $d = |\mathbf{r}_j - \mathbf{r}_i|$. For intra-site transitions due to symmetry considerations, $M_{ijm}^{\alpha,\beta}$ is zero whenever the difference between the angular momentum projections $l_\alpha - l_\beta$ is even and different from zero otherwise.

3.1. The normal state

We have calculated Eq. 1 for 1/8 of the FBZ at $T = 0K$; therefore, the Fermi functions were set equal to 1 for energies below or equal to the Fermi energy, E_F, and 0 otherwise. We show in Fig. 3 below three components of the optical conductivity tensor (Eq. 1), namely σ_{xx}, σ_{yy}, and σ_{zz} so that we can compare our results with those in the literature. Fig. 3 (top) shows our results for an energy interval from 1-10 eV. Fig. 3 (bottom) gives low-energy details (0-0.5 eV) of the three tensors. There is a clear anisotropy at low energies between σ_{xx} and σ_{yy}. This is due to transitions that take place on the chains (y-direction) that contribute to σ_{yy} but not to σ_{xx}. Garriga *et al.* [52] report measurements on $\varepsilon_2(\omega)$ which show a maximum around $\omega = 8eV$, a peak at $4 - 5eV$ and a minimum around $2 - 3eV$. Tajima *et al.* [53] report similar results at high energies and a minimum around 6 eV. Our calculation agrees well with these experimental results and with theoretical calculations at low energy [54] and at medium and high energies [55, 56].
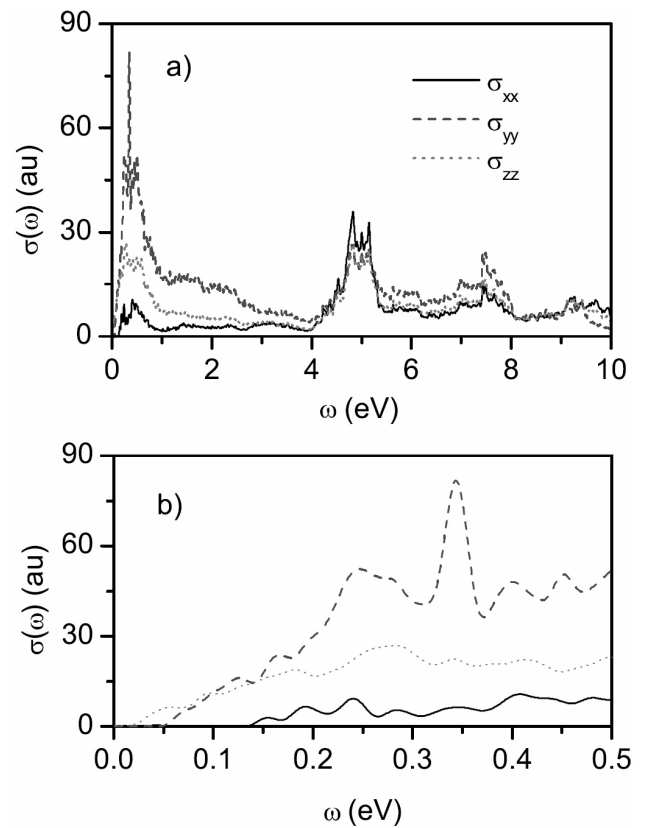
FIGURE 3. In the upper part (a), we show the optical conductivity-tensor components σ_{xx}, σ_{yy}, and σ_{zz} in the normal state in a scale 0-10 meV. In the lower part (b), we show the same functions in more detail below 0.5 eV so that our results can be easily compared with the ones in the literature (see text).
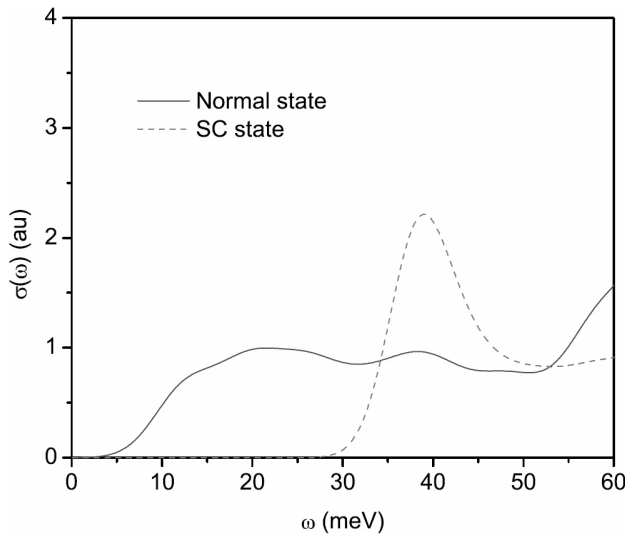
FIGURE 4. The optical conductivity function, $\sigma(\omega)$, in the normal (full line) and in the superconducting state (dots). Notice that at higher energies, $\sigma(\omega)$ increases with energy in the superconducting state.
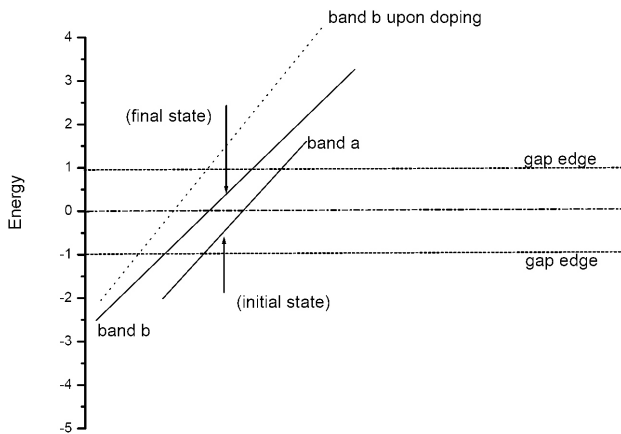
FIGURE 5. The dash-dot line is the Fermi energy and the dash-lines above and below it are the gap edge in the superconducting state. Let us consider transitions allowed in the normal state. In the band (a) we have selected a possible initial state (i) and on band (b) a possible final state. In normal state, this transition contributes to the resonance at a frequency equal to the energy difference between (f) and (i). In the superconducting state, both (f) and (i) will be projected to the gap edge so that this and several other low-lying similar transitions will all contribute at the same energy 2Δ due to the effect of the superconducting transition on the bands. Upon doping, it is enough for the bands to evolve so that their energy difference in the normal state gets higher than 2Δ at this pont of the FBZ (dot-line) for this particular event to cease to contribute to resonance (see text).

3.2. The superconducting state

We have calculated the optical conductivity from Eq. 1 for 1/8 of the FBZ with 64 points per axis. We have used our electronic band structure where a gap was inserted in the manner described above. We allow only inter-band transi-

tions in the in-CuO_2-plane states. Our result for $\sigma(\omega)$ in the normal and in the superconducting state appears in Fig. 4 below. As we can see in this figure, the effect of the transition is to shift the spectral weight of the almost featureless $\sigma(\omega)$ function to higher energies, namely above 30 meV, producing the sharp resonance at 38 meV. This occurs because all the allowed transitions within bands (one below and one above the Fermi level) that differ in the normal state by less than 2Δ are projected in the superconducting state on to the gap edges (above and below E_F), and the transition takes place at 2Δ regardless of the energy at which it occurs in the normal state. We have used $\Delta_{plane}=19$ meV for $YBa_2Cu_3O_7$. Both the calculation in the normal state and that in the superconducting state reproduce the experimental results. Our model does not assume any mechanism whatsoever. Therefore, an interesting point that arises is that, on quite general grounds, namely that the phase transition introduces a gapin to the electronic band structure, the resonance can be reproduced. This fact casts some doubt on whether or not the optical conductivity has enough information to permit a clear decision as to the mechanism (neither in the resonance nor in the background). This observation is actually consistent with the experiment by J. Hwang, T.Timusk and G.D. Gu [1].

4. Superconductivity with and without the resonance

A suggestion based as to our model on how the effect of doping can cause the total disappearance of resonance while the sample remains superconducting is sketched on Fig. 5. Let band (a) contain a possible initial state (i) below the Fermi energy, E_F (dash-dot line). Let the energy difference between state (i) and E_F be less than the gap associated with the plane, Δ_{plane} (dashed line). As the contributing transitions are inter-band, the final state has to lie on a different band (b) above the Fermi level. The transitions are direct (no momentum transfer). In the normal state, this transition contributes to the optical conductivity at a frequency equal to the energy difference between the final and the initial state. Several similar transitions would also occur but - and this is the key point - their contribution will cocur at different energies, in general. In the superconducting state, this and several similar events will contribute as well, but all at the same energy, namely, 2Δ due to the effect that the superconducting transition has on the bands. It is enough that, upon doping, a particular band should evolve in such a way that its energy (measured from the Fermi level) in the normal state becomes higher than 2Δ at the particular point of the FBZ where the allowed transition occurs, for this particular event to cease to contribute to the resonance in the superconducting state (see Fig. 5). It will contribute at a higher energy and, consequently, the resonance will have one less event that contributes, and its spectral weight diminishes. Eventually the resonance disappears. It is obvious, on the other hand, that, at a certain doping, bands that did not contribute at a previ-

ous one can contribute; but the net effect can be a losts of contributing events due to the doping. The exact issue depends on the details of the bands, on the specific influence of the doping on them and on the value of the gap for each family of compounds. Only an exact and detailed calculation can give an answer. We suggest that this is what happens in the Bi-family [1] where experiment shows the disappearance of the resonance with doping while superconductivity remains. Whenever, under doping, the gap shrinks at a slower pace than the number of events contributing to the resonance, the resonance disappears but superconductivity will remain.

5. Further remarks and Conclusions

We have shown in this letter that the resonance in the optical conductivity that appears in the superconducting and only in the superconducting state can be obtained from an *ab initio* three-dimensional calculation just by introducing in to the electronic bands that can be associated with the CuO_2 plane a gap, Δ. The actual calculation of the optical conductivity is two-dimensional (in-plane); nevertheless, it is worth noting that the bands contain information on the three-dimensional interactions. The model produces the resonance at 2Δ and we have consequently introduced into the calculation $\Delta = 19meV$ to reproduce the resonance at the right experimental frequency. The curves agree very well with experiment in the normal and the superconducting state. It is interesting that we get the experimental trend of the function at high frequency both in the normal and in the superconducting state. We do not assume any mechanism in our calculation. We have further suggested a way in which this model can account for the experimental results on the effect of doping on the intensity of the resonance [1].

It is important to mention that, using exactly the same model, we have calculated the spin polarized susceptibility in the normal and in the superconducting states and reproduced the experimental results. We find that the resonance in the spin-polarized susceptibility could disappear as well, but that there is no reason for it to do so at the same doping level as the one in the optical conductivity [47]. The model does not reproduce the experimental results for the tunneling experiments unless it is extended to three dimensions. If we further impose on the 3D bands obtained from our *ab initio* calculation, an additional gap to the states that can be associated with the chains ($\Delta_{chians} = 7meV$) and keep $\Delta = 0$ for the bands that can be associated with the c-axis, we reproduce the tunnelling characteristics of $YBa_2Cu_3O_7$ in agreement with experiment [48]. A somehow similar approach in the sense that they used a different value for the gap in each scenario (planes, chains and c-axis) has been used before [57] to successfully simulate experimental results on tunnelling, specific heat and ultrasonic attenuation. On that basis, we expect to reproduce these two last results as well from our more detailed model.

A more delicate point is to reproduce the temperature behavior of the resonance in the spin susceptibility. The resonance frequency hardly changes in the range from zero to the superconducting temperature but, on the contrary, its intensity is very sensitive to it; it decreases with increasing temperature and vanishes steeply at T_c [4]. We will suggest that this is a combined effect of the behavior of the superconducting gap with temperature and the separate effect of the increasing temperature on the electronic band structure itself. The effect of temperature on the electronic bands itself has never been considered before in this context but within the critical temperature range (≈ 100 K ≈ 10 meV); also, the temperature itself could have a non-negligible effect on the electronic band structure on the meV scale. Calculations of this effect in metals such as Cu and Ni have been made in the past by Delgadillo *et al.* [58]. They find that the electronic bands around the Fermi level do displace themselves as an effect of temperature in the meV scale. This fact, and the known temperature dependence of the superconducting gap itself, might explain (always within the same model) the behavior of the resonance with temperature. Notice that 10 meV is of the order of $\Delta/2$, where Δ is the superconducting gap associated with the CuO_2 plane [59].

The goal of the work presented in this and some other papers is to show how far one can go in describing the experimental results starting from what could be called "the result" of a theory of superconductivity for high-Tc superconductors. One possible conclusion is that the detailed description of the carriers plays the most important role in HTSC, a fact that is in sharp contrast with conventional superconductivity where the electronic band structure characteristics enter merely through the density of states at the Fermi energy.

A final question remains. Is this model a correct treatment of the superconducting transition? The answer to this is that the reproduction of many experimental results from one single hypothesis is, to say the least, intriguing. The use of Eliashberg gap equations assumes that, first, the mechanism is known and, second, that the mean field approximation holds. The extensive use of the several formulations based on the Hubbard Hamiltonian even beyond the mean field approximation, in spite of the fact that it reproduces an important number of experimental results, has not been conclusive since no ultimate explanation of the superconducting state has yet been achieved. This model uses solely a general property of the superconducting state avoiding any reference to the mechanism. We just directly calculate its consequences for thermodynamics. It turns out that we can reproduce important thermodynamic functions and give a panorama of the experimental trends where there is not much work in the literature.

The main conslusion seems to be that an accurate treatment of the electronic bands might play a role and that, for certain thermodynamic functions as tunnelling, for example, the problem can be formulated quite naturally and simply by just taking into account the three known scenarios [47,48,57].

1. J. Hwang, T. Timusk, and G.D. Gu, *Nature* **427** (2004) 714.

2. J. Rossat-Mignod *et al.*, *Physica C* **185-189** (1991) 86.

3. Phillip Bourges, in *The gap symmetry and Fluctuations in High Temperature Superconductors,* edited by J. Bok, G. Deutscher, D. Pavuna, and S.A. Wolf (Plenum Press, 1998).

4. Y. Sidis *et al.*, cond-mat/0401328 and references therein.

5. J.P. Carbotte, E Schachinger, and D.N. Basov, *Nature (London)* **401** (1999) 354.

6. J.M. Daams, J.P. Carbotte ,and R. Baquero, *J. Low Temp. Phys.* **35** (1979) 547; R. Baquero, J.M. Daams, and J.P. Carbotte, *J. Low Temp. Phys.* **42** (1981) 585.

7. F. Marsiglio, T. Startseva, and J.P. Carbotte, *Phys. Lett. A* **245** (1998) 172; F. Marsiglio, *J. Supercond.* **12** (1999) 163.

8. H.A. Mook *et al.*, *Nature* **395** (1998) 580.

9. H.F. Fong *et al., Nature* **398** (1999) 588.

10. H. He *et al., Phys. Rev. Lett.* **86** (2001) 1610.

11. A. Kaminski *et al., Phys Rev. Lett.* **86** (2001) 1070.

12. P.D. Johnson *et al., Phys. Rev. Lett.* **87** (2001) 177007.

13. M.R. Norman and H. Ding, *Phys. Rev. B* **57** (1998) R11089.

14. J.C. Campuzano *et al., Phys. Rev. Lett.* **83** (1999) 3709.

15. Ar. Abanov *et al., Phys. Rev. Lett.* **83** (1999) 1652.

16. J.F. Zasadzinski *et al.,* Phys. Rev. Lett. **87** (2001) 067005.

17. G.A. Thomas *et al.,*Phys. Rev. Lett. **61**, 1313 (1988).

18. A.V. Puchkov *et al.,* Phys. Rev. Lett. **61**, 3212 (1996).

19. D. Munzar, C. Bernhard, and M. Cardona, *Physica C* **317-318** (1999) 547.

20. A. Lanzara *et al., Nature* **412** (2001) 510.

21. P. Dai *et al., Nature* **406** (2000) 965.

22. E. Demler and Z.C. Zhang, *Nature* **396** (1998) 733.

23. D.J. Scalapino, *Science* **284** (1999) 1282.

24. G.H. Gweon, S.Y. Zhou, and A. Lanzara, cond-mat/0408475.

25. E. Schachinger, J.J. Tu, and J.P. Carbotte, *Phys. Rev. B* **67** (2003) 214505.

26. A. Rubio-Ponce, PhD Thesis, CINVESTAV, Mexico D.F. (1999), unpublished.

27. A. Rubio-Ponce and R. Baquero, *Rev. Mex. Fís.* **47** (2001) 447.

28. F. Puch, PhD Thesis, CINVESTAV, Mexico D.F. (2003), unpublished.

29. W.A. Harrison, *Solid State Theory* (Mc Graw-Hill, New York).

30. R. Baquero, to be published.

31. Norman, *Nature* **427** (2004) 692.

32. J.C. Phillips, cond-mat/0102108.

33. M.J. De Weert, D.A. Papaconstantopoulos, and W.E. Pickett, *Phys. Rev. B* **39** (1989) 4235.

34. W.E. Pickett, *Rev. Mod. Phys.* **61** (1989) 433.

35. F. Herman, R.V. Kaspwski, and W.Y. Hsu, *Phys. Rev. B* **36** (1987) 6904.

36. B. Szpunar and V.H. Smith Jr., *Phys. Rev. B* **37** (1988) 7525.

37. G.Y. Guo and W.M. Temmerman, *Phys. Rev. B* **41** (1990) 6372.

38. J.C. Slater and G.F. Koster, *Phys. Rev.* **94** (1954) 1498.

39. W.E. Pickett, R.E. Cohen, and H. Krakauer, *Phys. Rev. B* **42** (1990) 8764.

40. O.K. Andersen *et al.* Physica C **185-189**, 147 (1999).

41. S. Massida *et al.* Phys. Rev. Lett. A **122** (1987) 198.

42. A.A. Abrikosov, *Phys. Rev. Lett.* **73** (1994) 3302.

43. A.A. Abrikosov, J.C. Campuzano, and K. Gofron, *Physica C* **214** (1993) 73.

44. E. López-Hernández PhD Thesis, CINVESTAV, Mexico D.F. (1997), unpublished.

45. D.J. Chadi and M.L. Cohen, *Phys. Rev. B* **8** (1973) 5747.

46. G. Gilat and N.R. Bharatiya, *Phys. Rev. B* **12** (1975) 3479.

47. R. Baquero *et al.*, sent to *European Physical Journal.*

48. R. Baquero *et al.*, sent to *Phys. Rev. B.*

49. J.R. Schrieffer, *Theory of Superconductivity*, W.A. Benjamin, INC., Reading, Ma. (1964); N. Bulut, and D.J. Scalapino, *Phys. Rev. B* **53** (1996) 5149.

50. F. Puch and R. Baquero, to be published.

51. W.A. Harrison, *Electronic Structure and the Properties of Solids* (W.H. FreemN nd Company, USA, 1980).

52. M. Garriga, J. Humlicek, J. Barth, R.L. Johnson, and M. Cardona, *J. Opt. Soc. Am. B* **6** (1989) 470.

53. S. Tajima *et al., J. Opt. Soc. Am. B* **6** (1989) 475.

54. S.T. Chui, R.V. Rasowsky, and W.Y. Hsu, *Phys. Rev. Lett.* **61** (1988).

55. E.G. Maksimov, S.N. Rashkeev, S. Yu Savrasov, and Yu A. Uspenskii, *Phys. Rev. Lett.* **63** (1989).

56. Guang-lin Zhao, Y. Xu, and W. Y. Ching, *Phys. Rev. B* **36** (1987).

57. A.M. Cucolo, C. Noce, and A. Romano, *Phys. Rev. B* **53** (1996) 6764.

58. I. Delgadillo, H. Gollisch, and R. Feder, *Solid State Comm.* **88** (1993) 789.

59. R. Baquero *et al.*, sent to *J. of Superconductivity.*